Properties of the bound $\Lambda(\Sigma)NN$ system and hyperon-nucleon interactions

K. Miyagawa
Faculty of Liberal Arts and Science, Okayama University of Science, Ridai-cho, Okayama 700, Japan

H. Kamada and W. Glöckle
Institut für Theoretische Physik II, Ruhr Universität Bochum, 44780 Bochum, Germany

V. Stoks
School of Physical Sciences, The Flinders University of South Australia, Bedford Park, South Australia 5042, Australia
(Received 6 February 1995)

The Faddeev equations for the hypertriton are solved precisely using the Nijmegen hyperon-nucleon and realistic NN interactions. The hypertriton turns out to be bound at the experimental value. Thereby the Λ-Σ conversion is crucial. States of the $\Lambda(\Sigma)NN$ system with quantum numbers (T, J) different from $(0, \frac{1}{2})$ are not bound. We visualized properties of the hypertriton wave function in various ways.

PACS number(s): 21.80.+a, 21.45.+v

I. INTRODUCTION

The hypertriton (${}^{3}_{\Lambda}$H), the lowest mass hypernucleus, offers interesting studies for the strange-particle nuclear physics. It provides additional information for recently developed meson-theoretical YN forces, since the available YN scattering data are still extremely poor. It also serves as a laboratory to study Λ-Σ conversion. This has provoked many studies in the past based on simple forces and mostly variational estimates, which gave much qualitative insight. We refer the reader to our recent study [1] for references. In that article [1], we solved the Faddeev equations for the coupled ΛNN and ΣNN systems precisely, for meson-theoretical NN and YN interactions. Using the Jülich YN interaction in a one-boson-exchange (OBE) potential parametrization [2] (energy-independent version $\tilde{A}$) and various realistic NN interactions, the hypertriton turned out to be unbound. Here we repeat this study using another meson-theoretical YN interaction, namely that of the Nijmegen group [3]. This will give us a first indication about the spread in the theoretical predictions of the hypertriton binding energy based on present day meson-theoretical YN forces.

In the past [4] the question was posed whether states of total isospin and total angular momentum, other than $T = 0$ and $J = \frac{1}{2}$, are also bound. We shall investigate that question for the most natural candidates $T = 0$, $J = \frac{3}{2}$ and $T = 1$, $J = \frac{1}{2}$ or $\frac{3}{2}$.

The very weak binding energy of the hypertriton leads one to expect that the wave function is mostly a deuteron surrounded by a distant Λ particle. We analyze our exact wave function and visualize its properties in various manners in configuration space. This will be contrasted to corresponding properties of the triton.

In Sec. II we briefly review our formalism and present the results for the hypertriton using the Nijmegen YN interaction [3], together with various realistic NN forces. Section III is devoted to clarify the question whether states of T and J different from $T = 0$ and $J = \frac{1}{2}$ could be expected to be bound. Properties of the hypertriton wave function will be displayed in Sec. IV. We summarize and give a brief outlook in Sec. V.

II. THE HYPERTRITON WITH THE NIJMEGEN YN INTERACTION

We allow for the Λ-Σ conversion and consequently use a coupled-channel formalism. As shown in [1], one arrives at two coupled (matrix) Faddeev equations

$$\underline{\psi}^{(12)} = \frac{1}{E - \underline{H}_0}\, \underline{T}_{12}(1 - P_{12})\underline{\psi}^{(13)} ,$$
$$\underline{\psi}^{(13)} = \frac{1}{E - \underline{H}_0}\, \underline{T}_{13}(\underline{\psi}^{(12)} - P_{12}\underline{\psi}^{(13)}) . \qquad (1)$$

Each of the two Faddeev amplitudes has two components

$$\underline{\psi}^{(ij)} = \begin{pmatrix} \psi_{\Lambda}^{(ij)} \\ \psi_{\Sigma}^{(ij)} \end{pmatrix} , \qquad (2)$$

and the free propagator as well as the baryon-baryon $\underline{T}$ operators are 2×2 matrices. The nucleon-nucleon T matrix $\underline{T}_{12}$ is of course diagonal and only the inherent free propagator distinguishes the presence of a Λ or a Σ. The hyperon-nucleon T matrix $\underline{T}_{13}$, however, is full and incorporates the $\Lambda N \longleftrightarrow \Lambda N$, $\Sigma N \longleftrightarrow \Sigma N$, and the $\Lambda N \longleftrightarrow \Sigma N$ transitions. The two orthogonal parts of the total wave function are given as

$$\Psi_{NN\Lambda} = \psi_{\Lambda}^{(12)} + (1 - P_{12})\, \psi_{\Lambda}^{(13)} ,$$
$$\Psi_{NN\Sigma} = \psi_{\Sigma}^{(12)} + (1 - P_{12})\, \psi_{\Sigma}^{(13)} . \qquad (3)$$

Clearly, P_{12} is a nucleon-nucleon transposition operator. For more details of our notation and the technical per-

formance of solving the set precisely in momentum space and in a partial wave decomposition, we refer the reader to Ref. [1].

The set (1) can be put into the form

$$\eta(E)\underline{\psi} = \underline{K}(E)\underline{\psi} , \tag{4}$$

with $\eta(E) = 1$ at the hypertriton binding energy. Let us choose the energy E to be zero at the ΛNN threshold. Then a bound state exists if an eigenvalue $\eta(E) = 1$ can be found below the Λd threshold at −2.225 MeV.

We evaluated $\eta(E)$ at three energies $E = -2.5, -2.4$, and -2.3 MeV, respectively, for various truncations in the number of partial wave states, usually called channels in this context. The number of channels can be ordered by assuming that the YN and NN forces act only up to certain states. Thus, one has 15 channels keeping the forces different from zero only in the states $^1S_0$ and $^3S_1$-$^3D_1$, 30 channels if all force components are kept up to $j = 1$, and 54, 78, and 102 channels if the forces are kept up to $j = 2$, 3, and 4, respectively. We refer the reader to [1], where the quantum numbers for the first 15 channels have been displayed. As an example, which might be helpful also for later work by other groups, we display in Table I the convergence of $\eta(E)$ at $E = -2.4$ MeV, increasing the number of channels. In this example the updated Nijmegen 93 NN potential [5] is used. We see convergence. Corresponding calculations for other realistic NN potentials generate very similar results and there is not much dependence on the choice of the NN force. All forces should be of course realistic in the sense that they describe the deuteron properties and the NN phase shifts (NN scattering data) about equally well.

In Fig. 1 we show the energy dependence of the eigenvalue $\eta(E)$ below the Λd threshold for the Nijmegen YN and NN forces. The momentum-space versions of these Nijmegen potentials are exactly equivalent to the configuration-space versions and the detailed expressions for the partial-wave Nijmegen potentials in momentum space are given in Ref. [6]. For all other NN forces used the curves are very close to the one shown. It turns out that for all choices of the NN forces used the hypertriton is bound: for Bonn B [7] at −2.37 MeV, for Paris [8] at −2.36 MeV, and for Nijmegen 93 [5] at −2.36 MeV, respectively. The differences in binding energies are very small, about 10 keV at most. A similar result we also found in [1], estimating the binding energies for the Jülich YN interaction (properly enhanced, since the

TABLE I. The eigenvalue $\eta(E)$ of the Faddeev kernel at $E = -2.4$ MeV for an increasing number of channels. The Nijmegen YN [3] and the Nijmegen 93 NN [5] potentials have been used.

Channels	η ($E = 2.4$ MeV)
15 ch	0.984
30 ch	0.973
54 ch	0.985
78 ch	0.989
102 ch	0.989

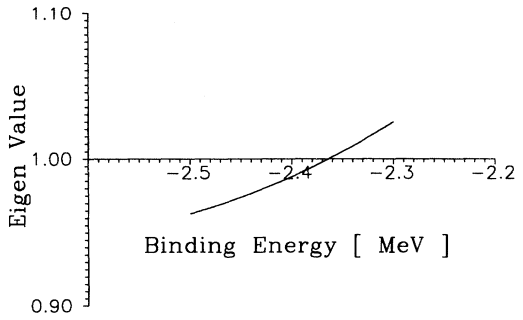

FIG. 1. The energy dependence of the eigenvalues $\eta(E)$ for the Nijmegen 93 NN and the Nijmegen YN interactions. The curves for the other NN potentials essentially overlap with the curve shown.

Jülich YN interaction as it stands does not bind the hypertriton). Again the NN potential, Bonn B, with the smallest deuteron D-state probability binds strongest.

All three theoretical binding energies for Bonn B, Paris, and Nijmegen are within the experimental errors of -2.35 ± 0.05 MeV. In two previous reports [9,10], we used a preliminary version of the Nijmegen YN interaction [11] together with the Paris NN potential, which yielded −2.37 MeV hypertriton binding energy.

The wave function (3) consists of two orthogonal parts, (ΛNN) and (ΣNN), and one can determine the probability of finding a Λ or a Σ in the hypertriton. We get for the Nijmegen YN and the Nijmegen 93 NN interaction

$$\begin{aligned} P_\Lambda &= 0.995 , \\ P_\Sigma &= 0.005 . \end{aligned} \tag{5}$$

Thus, a "measurement" would find most of the time the hyperon to be a Λ particle. The results for other NN potentials are very much the same.

It is also of interest to break the total potential and kinetic energies apart:

$$\begin{aligned} \langle V \rangle &= \langle V_{NN} \rangle + \langle V_{YN} \rangle , \\ \langle V_{NN} \rangle &= \langle V_{NN} \rangle_\Lambda + \langle V_{NN} \rangle_\Sigma , \\ \langle V_{YN} \rangle &= \langle V_{\Lambda N,\Lambda N} \rangle + \langle V_{\Lambda N,\Sigma N} \rangle \\ &\quad + \langle V_{\Sigma N,\Lambda N} \rangle + \langle V_{\Sigma N,\Sigma N} \rangle , \\ \langle T \rangle &= \langle T_{NN} \rangle + \langle T_{Y-NN} \rangle , \\ \langle T_{NN} \rangle &= \langle T_{NN} \rangle_\Lambda + \langle T_{NN} \rangle_\Sigma , \\ \langle T_{Y-NN} \rangle &= \langle T_{\Lambda-NN} \rangle + \langle T_{\Sigma-NN} \rangle . \end{aligned} \tag{6}$$

Of course, the expectation values of the YN interactions include the factor 2 resulting from the two nucleons. The results are displayed in Table II. The total potential energy is $\langle V \rangle = -25.80$ MeV and the total kinetic energy is $\langle T \rangle = 23.45$ MeV. The very naive expectation might have been that the pure nucleon parts of $\langle T \rangle$ and $\langle V \rangle$, given by 20.48 MeV and −22.25 MeV, respectively, are very close to the values of the free deuteron, which for Nijmegen 93 are $\langle T \rangle_d = 19.304$ and $\langle V \rangle_d = -21.528$ MeV, respec-

TABLE II. The various kinetic and potential energy contributions of Eqs. (6) in the hypertriton, using the Nijmegen *YN* and Nijmegen 93 *NN* interactions. The potential energy of the hyperon-nucleon interaction is broken up further into its contribution from the states $^1S_0$ and $^3S_1$-$^3D_1$. All numbers are in units of MeV.

Partial wave	$\langle V_{\Lambda N,\Lambda N}\rangle$	$\langle V_{\Lambda N,\Sigma N}\rangle$	$\langle V_{\Sigma N,\Lambda N}\rangle$	$\langle V_{\Sigma N,\Sigma N}\rangle$	$\langle V_{YN}\rangle$
$^1S_0$	-1.60	-0.19	-0.19	0.03	-1.95
$^3S_1$-$^3D_1$	0.02	-0.77	-0.77	-0.06	-1.57
all	-1.58	-0.97	-0.97	-0.02	-3.54
	$\langle V_{NN}\rangle_\Lambda$	$\langle V_{NN}\rangle_\Sigma$			$\langle V_{NN}\rangle$
all	-22.22	-0.03			-22.25
	$\langle T_{NN}\rangle_\Lambda$	$\langle T_{NN}\rangle_\Sigma$			$\langle T_{NN}\rangle$
all	20.25	0.23			20.48
	$\langle T_{\Lambda-NN}\rangle$	$\langle T_{\Sigma-NN}\rangle$			$\langle T_{Y-NN}\rangle$
all	2.18	0.79			2.97

tively. They are indeed close, but not close enough, and $\langle V_{NN}\rangle + \langle T_{NN}\rangle$ add up to −1.77 MeV only, not to the deuteron binding energy. This means that the two nucleons in the hypertriton do not sit all the time in the state of the deuteron, but also in energetically higher states. The remaining binding energy of −0.57 MeV comes from the hyperon, as displayed in Table II. It is interesting to see from Table II that the Λ particle alone brings in more kinetic energy than the magnitude of its potential energy. It is only due to the Λ-Σ conversion that the potential energy of the hyperon wins and that the hyperon provides −0.57 MeV binding energy. We would like to note that $\langle T_{\Sigma-NN}\rangle$ in Table II includes the mass difference of +78 MeV between Σ and Λ, and in fact about half of the number given results from that mass difference.

Finally it is of interest to see the contributions of the $^1S_0$ and $^3S_1$-$^3D_1$ *YN* force components to the potential energy separately. It results in

$$\langle V_{YN}\rangle^{^1S_0} = -1.95 \text{ MeV} ,$$
$$\langle V_{YN}\rangle^{^3S_1-^3D_1} = -1.57 \text{ MeV} . \quad (7)$$

The ratio of these numbers is quite different from the estimated factor 3, which is quoted very often in the literature. Again, these numbers build up in an interesting manner linked to the Λ-Σ conversion. This is also displayed in Table II. Thus, $\langle V_{\Lambda N,\Lambda N}\rangle$ comes nearly fully from $^1S_0$ alone, while the Λ-Σ transition matrix elements receive their dominant contribution in the state $^3S_1$-$^3D_1$.

Let us add now some comments about the outcomes for the three different *YN* interactions used up to now. While the Jülich *YN* interaction does not lead to a bound hypertriton, the preliminary and final Nijmegen interactions do. An important *YN* force component is $^1S_0$. We display in Fig. 2 the partial total cross sections for Λ*N* scattering based on the $^1S_0$ and $^3S_1$-$^3D_1$ interactions for the Jülich and the Nijmegen potentials, respectively. We see that for the very low energies the Nijmegen curve for the $^1S_0$ contribution is larger than the Jülich curve. The curves for the final Nijmegen potential are close to the ones of the preliminary Nijmegen potential. We shall see below that the average kinetic energy of the Λ particle in the hypertriton is 2.18 MeV, which emphasizes the importance of the very low energies, where the $^1S_0$ Nijmegen potentials are more attractive than the Jülich potential. This can also be seen in the scattering lengths shown in Table III.

The total cross sections for the three *YN* potentials using all relevant partial waves are shown in Fig. 3 in comparison to the few poor data points [12,13]. Apparently, these data cannot be used to rule out any of the three potential predictions.

It is possible that the stronger attraction of the $^1S_0$ Nijmegen potential at the very low energies is responsible for the fact that it binds the hypertriton, while the Jülich one with less attraction does not bind. At least part of the reason might also lie in the very different Λ-Σ conversion potentials, as will be discussed now.

Does the Jülich *YN* interaction in the hypertriton lead to similar numbers as in Table II? This is not obvious, since we already found in [1] that the binding there is mostly dependent on the $^1S_0$ *YN* force and much less

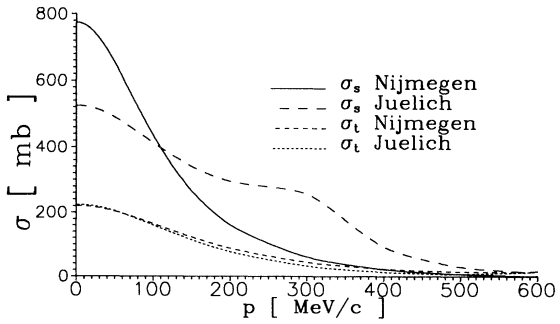

FIG. 2. The partial total Λ*N* cross sections σ_s and σ_t to the states $^1S_0$ and $^3S_1$, respectively, where the total cross section is $\sigma_{\rm tot} = \frac{3}{4}\sigma_t + \frac{1}{4}\sigma_s$. Comparison of the Nijmegen and Jülich *YN* interactions.

TABLE III. The $^1S_0$ and $^3S_1$ scattering lengths (in fm) for the preliminary Nijmegen [11], final Nijmegen [3], and the Jülich [2] *YN* interactions, respectively.

Potential (ΛN)	$^1S_0$	$^3S_1$
Nijmegen [3]	-2.48	-1.32
Jülich [2]	-2.04	-1.33
Nijmegen (modified) [11]	-2.45	-1.51

on the $^3S_1$-$^3D_1$ *YN* force, which is in contrast to what we found for the Nijmegen *YN* interaction. This can be seen quantitatively by the fact that one has to multiply either the $^1S_0$ Jülich *YN* force by a factor 1.045 to get the correct hypertriton binding energy, or the $^3S_1$-$^3D_1$ *YN* force by a factor 1.25. Now in order to generate numbers corresponding to Table II for the Jülich case, we have first of all to generate artificially a bound hypertriton at the correct binding energy. To that aim we enhance both the $^1S_0$ and $^3S_1$-$^3D_1$ *YN* forces by the factor 1.041. Thereby the *NN* potential is chosen to be Bonn B. Using that hypertriton wave function we determine all the expectation values as in Table II. The results, shown in Table IV, are strikingly different from the ones for the Nijmegen interactions. The total *YN* potential energy in the Jülich case is much larger and the contribution from the Σ and the Λ-Σ transition is much bigger than in the Nijmegen case. Furthermore, the $^1S_0$ part for the Λ alone is repulsive and overrides the attractive part in the state $^3S_1$-$^3D_1$. Thus, altogether the Λ part by itself is repulsive. The kinetic and potential energy of the two nucleons are also quite different. The two nucleons by themselves would not even be bound, which is strikingly different from the Nijmegen case. Finally, since the probability to find the Σ is 0.042, roughly a factor of 10 larger than in the Nijmegen case, also the kinetic energy (including the rest mass difference) of the Σ is much larger than in the Nijmegen case. The comparison of Tables II and IV clearly shows that the two present-day *YN* interactions, both based on meson exchanges, are still quite apart from each other.

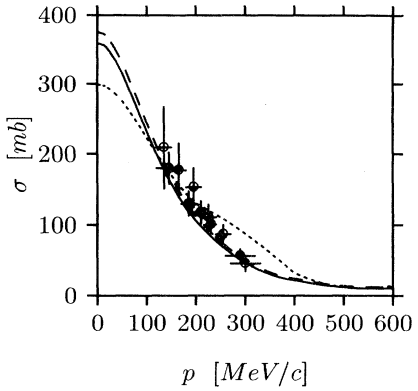

FIG. 3. The total ΛN cross section data (solid circle [12] and open circle [13]) in comparison to the three *YN* potential predictions: preliminary Nijmegen [11] (solid), final Nijmegen [3] (dashed), and Jülich [2] (dotted).

Finally, let us investigate the polarizations of the Λ and Σ particles inside a polarized hypertriton. They are defined by

$$P(\Lambda,\Sigma) \equiv \langle \Psi m = \tfrac{1}{2} | \tfrac{1}{2}\sigma_z(\Lambda,\Sigma) | \Psi m = \tfrac{1}{2} \rangle \qquad (8)$$

and we find

$$P(\Lambda) = -0.166\ ,$$
$$P(\Sigma) = 0.001\ . \qquad (9)$$

The Σ polarization had trivially to be small because of the low probability to find a Σ. The small Λ polarization is a dynamic effect and results, roughly spoken, from the interference with the spin 1 of the deuteron. The number –0.166 tells that the probability to find the Λ spin downward $(-\frac{1}{2})$ is about 2/3, and to find it upward is about 1/3.

TABLE IV. The various kinetic and potential energy contributions of Eqs. (6) in the hypertriton, using the Jülich *YN* (properly enhanced) and the Bonn B *NN* interactions. The potential energy of the hyperon-nucleon interaction is broken up further into its contribution from the states $^1S_0$ and $^3S_1$-$^3D_1$. All numbers are in units of MeV.

Partial wave	$\langle V_{\Lambda N,\Lambda N}\rangle$	$\langle V_{\Lambda N,\Sigma N}\rangle$	$\langle V_{\Sigma N,\Lambda N}\rangle$	$\langle V_{\Sigma N,\Sigma N}\rangle$	$\langle V_{YN}\rangle$
$^1S_0$	2.65	-4.23	-4.23	-5.61	-11.42
$^3S_1 - ^3D_1$	-0.66	-0.32	-0.32	-0.07	-1.36
all	1.99	-4.54	-4.54	-5.68	-12.78
	$\langle V_{NN}\rangle_\Lambda$	$\langle V_{NN}\rangle_\Sigma$			$\langle V_{NN}\rangle$
all	-17.34	-0.17			-17.51
	$\langle T_{NN}\rangle_\Lambda$	$\langle T_{NN}\rangle_\Sigma$			$\langle T_{NN}\rangle$
all	15.47	2.14			17.61
	$\langle T_{\Lambda-NN}\rangle$	$\langle T_{\Sigma-NN}\rangle$			$\langle T_{Y-NN}\rangle$
all	2.17	8.16			10.33

III. STATES WITH DIFFERENT QUANTUM NUMBERS

In the past [4] the Λ*NN* system was investigated not only in the state of total isospin $T = 0$ and total angular momentum $J = \frac{1}{2}$ but also for $T = 0, J = \frac{3}{2}$. There were also discussions about different three-body force effects resulting from the Λ-Σ conversion in different states (attractive and repulsive ones). Based on the modern meson-theoretical hyperon-nucleon and nucleon-nucleon interactions, it is clear from the previous work [1] and the present one that three-body force effects resulting from Λ-Σ conversion are attractive in the state $J = 0, T = \frac{1}{2}$.

Now let us regard the states with total isospin and angular momenta $T = 0, J = \frac{3}{2}$ and $T = 1, J = \frac{1}{2}$ or $\frac{3}{2}$. This leads to different channel quantum numbers in comparison to the state $T = 0, J = \frac{1}{2}$, for which the most important ones have been displayed in [1]. The new most important ones are shown in Table V. As in [1], they are grouped into two parts, belonging either to the basis states

$$|pq\alpha r\rangle \equiv |pq(ls)j(\lambda\tfrac{1}{2})I(jI)J(tt_r)T\rangle \tag{10}$$

or

$$|pq\beta r\rangle \equiv |pq(ls)j(\lambda\tfrac{1}{2})I(jI)J[(t_r\tfrac{1}{2})t\tfrac{1}{2}]T\rangle \ . \tag{11}$$

In the case of the $\alpha(\beta)$ states the two-body subsystem consists of $2N$ (hyperon + N) and the spectator is a hyperon (N). The quantum numbers of the two-body subsystem are the relative momentum p and the obvious quantum numbers $(ls)j$, and for the third particle the relative momentum q and $(\lambda\frac{1}{2})I$. Finally, j and I are coupled to the total three-body angular momentum J. The index r distinguishes between Λ and Σ. For the α states the hyperon is the third particle, while in the β states it belongs to the two-body subsystem. This explains the coupling scheme for the total isospin T. For more details, see Ref. [1]. Table V does not include the β states, where t for the ΣN subsystem has the value $\frac{3}{2}$. We included them in the calculation, but their contribution is very small.

We solved the eigenvalue problems below the Λd threshold for the $T = 0$ state and below the Λ*NN* threshold for the $T = 1$ states. It turned out that they are not bound. Therefore, we multiplied the total *YN* interaction by strength factors f such that the states are bound. This provides a feeling for how much one is away from a situation where binding would occur. The results for f are displayed in Fig. 4 for two energies and two states (T, J) under consideration. We used the Nijmegen *YN* interaction and the Bonn B *NN* interaction. Figure 4 tells that the Λ(Σ)*NN* system based on the present day meson-theoretical interactions would only be bound in these two states if the *YN* interaction would be enhanced by more than 20%. For the state $T = 1, J = \frac{3}{2}^+$, we could not find a three-body bound state up to the strength factor 1.32, where the Nijmegen *YN* $^3S_1$-$^3D_1$ force supports a two-body bound state. There is only one bound state for the Λ(Σ)*NN* system for $T = 0$ and $J = \frac{1}{2}$.

While writing this article, a similar study occurred [14] on the $(T = 2, J = \frac{1}{2})$ and $(T = 2, J = \frac{3}{2})$ states. There the enhancement factor for the Jülich *YN* interaction turned out to be larger than 1.7.

We also checked those three-body force effects which

TABLE V. The most important channel quantum numbers for the Faddeev amplitudes for the states $(T = 0, J = \frac{3}{2}^+)$, $(T = 1, J = \frac{1}{2}^+)$, and $(T = 1, J = \frac{3}{2}^+)$. The α and β states refer to the basis states (10) and (11) and are separated by a line, the α states being the upper group. The β states come twice, since the hyperon can be either the Λ particle ($t_r = 0$) or the Σ particle ($t_r = 1$).

			$J = \frac{3}{2}^+, T = 0$			
l	s	j	λ	$2I$	$2t$	$2t_r$
0	1	1	0	1	0	0
2	1	1	0	1	0	0
0	1	1	2	3	0	0
2	1	1	2	3	0	0
0	1	1	2	5	0	0
2	1	1	2	5	0	0
0	0	0	2	3	2	2
0	0	0	2	3	1	0 or 2
0	1	1	0	1	1	0 or 2
2	1	1	0	1	1	0 or 2
0	1	1	2	3	1	0 or 2
2	1	1	2	3	1	0 or 2
0	1	1	2	5	1	0 or 2
2	1	1	2	5	1	0 or 2
			$J = \frac{1}{2}^+, T = 1$			
l	s	j	λ	$2I$	$2t$	$2t_r$
0	0	0	0	1	2	0
0	0	0	0	1	2	2
0	1	1	0	1	0	2
2	1	1	0	1	0	2
0	1	1	2	3	0	2
2	1	1	2	3	0	2
0	0	0	0	1	1	0 or 2
0	1	1	0	1	1	0 or 2
2	1	1	0	1	1	0 or 2
0	1	1	2	3	1	0 or 2
2	1	1	2	3	1	0 or 2
			$J = \frac{3}{2}^+, T = 1$			
l	s	j	λ	$2I$	$2t$	$2t_r$
0	0	0	2	3	2	0
0	0	0	2	3	2	2
0	1	1	0	1	0	2
2	1	1	0	1	0	2
0	1	1	2	3	0	2
2	1	1	2	3	0	2
0	1	1	2	5	0	2
2	1	1	2	5	0	2
0	0	0	2	3	1	0 or 2
0	1	1	0	1	1	0 or 2
2	1	1	0	1	1	0 or 2
0	1	1	2	3	1	0 or 2
2	1	1	2	3	1	0 or 2
0	1	1	2	5	1	0 or 2
2	1	1	2	5	1	0 or 2

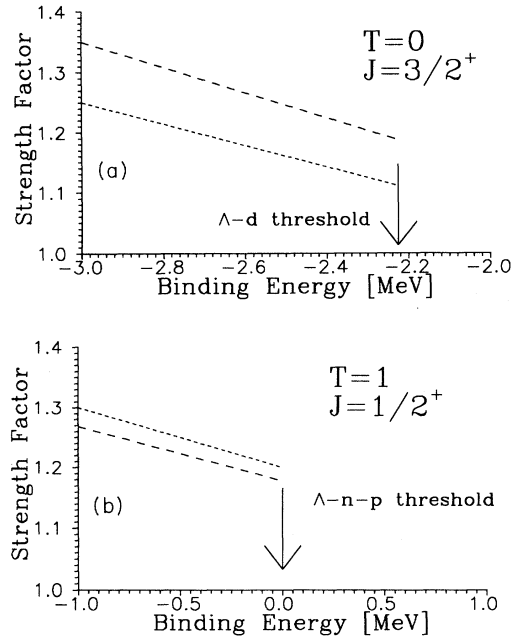

FIG. 4. The enhancement factors f (long dashed) multiplying the Nijmegen YN interaction necessary to bind the $\Lambda(\Sigma)NN$ system for the states (T, J) equal to (a) $(0, \frac{3}{2}^+)$ and (b) $(1, \frac{1}{2}^+)$. The short dashed lines result if the transition t matrix elements $t_{N\Lambda,N\Sigma}$ are switched off (see text).

result from turning off the $t_{N\Lambda,N\Sigma}$ matrix elements of the two-nucleon t matrix in the three-body system, keeping them however in the two-body system. This excludes ΣNN states between consecutive t operations and one stays therefore always in the space of ΛNN states. The results are also displayed in Fig. 4 for two cases $T = 0, J = \frac{3}{2}$ and $T = 1, J = \frac{1}{2}$. We find for $T = 0, J = \frac{3}{2}^+$ that turning off the transition t matrices requires a decrease of the strength factor. Therefore, allowing for the transitions to the ΣNN system provides a repulsion. For the other state $T = 1, J = \frac{1}{2}^+$ one has attraction like in the hypertriton ground state. It might be also of interest to note that in the state $T = 0, J = \frac{3}{2}^+$ the YN $^1S_0$ force has essentially negligible effect.

IV. VISUALIZATION OF THE HYPERTRITON WAVE FUNCTION

First we would like to find the most probable spatial configuration of the two nucleons and the hyperon inside the hypertriton. Such a study has already been undertaken for the three nucleons in the triton [15]. The spatial positions of the three baryons always define a plane. Let us locate the hyperon and the center of mass of the hypertriton on the positive z axis in that plane, say. For a given position of the hyperon we can search for that location of one of the nucleons such that the value of the wave function is maximal. For each choice of the location of one of the nucleons the location of the second nucleon is automatically given, since the center-of-mass position is fixed. Having found the position of the nucleon for which the wave function is maximal one can repeat that search for another location of the hyperon on the positive z axis until one reaches the absolute maximum. This defines the most probable geometrical configuration of the three baryons inside the hypertriton. This is displayed in Fig. 5 for the two cases that the hyperon is the Λ particle or the Σ particle. The configurations are totally different. While the Σ is very close to one or the other nucleon (a linear configuration), the Λ particle is further apart from the nucleons than the nucleons from each other. This reflects of course the different separation energies, 150 keV for the Λ particle and 150 keV + 78 MeV (the mass difference of Σ and Λ) for the Σ particle. In the triton the triangle formed by the three nucleons is nearly equilateral (see Ref. [15]). The triangle formed by the Λ and the two nucleons is somewhat prolongated in the direction where the Λ particle is sitting, and the maximum in the wave function is rather flat. In the case of ΣNN the Σ sits not in the middle between the two nucleons but close to one or the other nucleon. Of course, that part of the wave function is much smaller than the one for ΛNN.

It is interesting to see how the wave function drops if one goes away from that most probable geometrical arrangement. This is shown in Figs. 6 and 7 for the

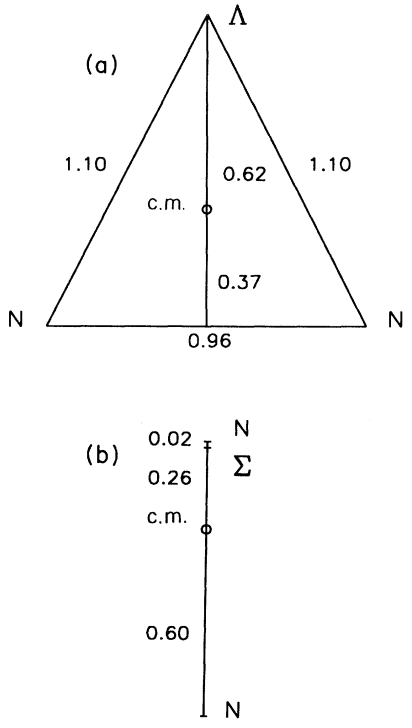

FIG. 5. The most probable geometric configuration for (a) the ΛNN system and (b) the ΣNN system in the hypertriton. Note that the Σ can sit either close to one or the other nucleon with equal probability. (Only one of the two possibilities is shown.)

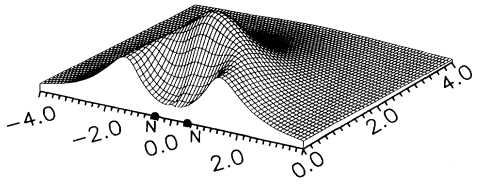

FIG. 6. The magnitude squared of the hypertriton wave function for fixed positions of the two nucleons (the most probable ones of Fig. 5), as a function of the location of the Λ particle. The units of the axis are in fm.

Λ*NN* and Σ*NN* cases, respectively. In these figures the nucleons are fixed at their most probable sites, like in Fig. 5. We see that in contrast to the third nucleon in the triton [15], the Λ has also a high probability to approach the two nucleons. For the Σ the probability is strongly peaked around the nucleon and then drops very quickly in the direction perpendicular to the line connecting the two nucleons.

The total wave function depends on the magnetic spin quantum numbers of the three baryons. Therefore, we can ask more detailed questions. For the hypertriton polarized upward, the spin orientations of the two nucleons averaged, and the Λ particle polarized downward or upwards, the probabilities for the Λ positions are shown in Fig. 8. They are quite different: high along a bended ridge or concentrated in a peak. The two pictures added up give back the total probability shown in Fig. 6.

Though the probabilities for the Σ part of the wave function are very small, we would like to display nevertheless the interesting corresponding cases for different spin directions. For the total spin of the Σ*NN* system pointing upward, and summing independently over the spin directions of the two nucleons, the wave function is peaked for a collinear (triangular) configuration if the spin of the Σ particle points upward (downward), as shown in Fig. 9. An even more detailed situation is displayed in Fig. 10, where the nucleon spins are chosen to be opposite. Then it turns out that the Σ with spin upward prefers to stay close to that nucleon with spin downward.

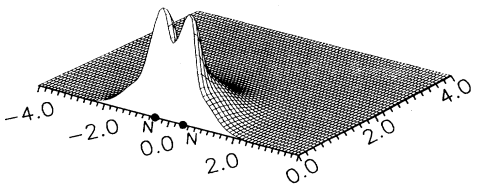

FIG. 7. The magnitude squared of the hypertriton wave function for fixed positions of the two nucleons (the most probable ones of Fig. 5), as a function of the location of the Σ particle. The wave function squared is multiplied by a factor of 10 in relation to the values in Fig. 6. The units of the axis are in fm.

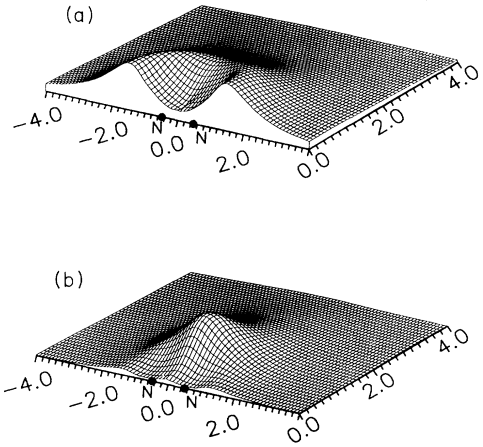

FIG. 8. The magnitude squared of the wave function for the hypertriton, polarized upward and averaged over the polarizations of the two nucleons for the cases that the Λ is polarized (a) downward and (b) upward. The units of the axis are in fm.

Let us now probe the hypertriton wave function in a different manner. In contrast to the triton, one has to expect that the two nucleons in the hypertriton have a large probability to be found in the state of the deuteron. We evaluated the overlap of the deuteron with the hypertriton and triton wave functions, respectively:

$$\rho_d(r) \equiv \frac{1}{2} \sum_{m_d m M} |\langle \phi_d m_d \vec{r} m | \Psi M \rangle|^2 \ . \tag{12}$$

Here $\vec{r}$ denotes the distance of the third particle (Λ or Σ in the hypertriton, neutron in the triton) from the center of mass. In case of the triton we have chosen a 34-channel Faddeev wave function for the Bonn B *NN*

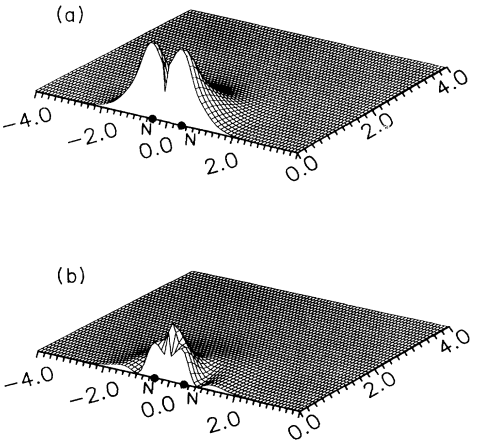

FIG. 9. Same as in Fig. 8 for the Σ part of the hypertriton wave function. The units of the axis are in fm.

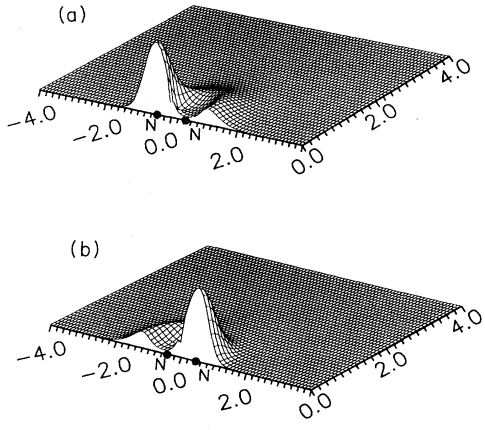

FIG. 10. The magnitude squared of the Σ part of the wave function of the hypertriton (polarized upward) and the left nucleon, the Σ particle, and the right nucleon polarized as (a) downward, upward, upward and (b) upwards, upward, downward. The units of the axis are in fm.

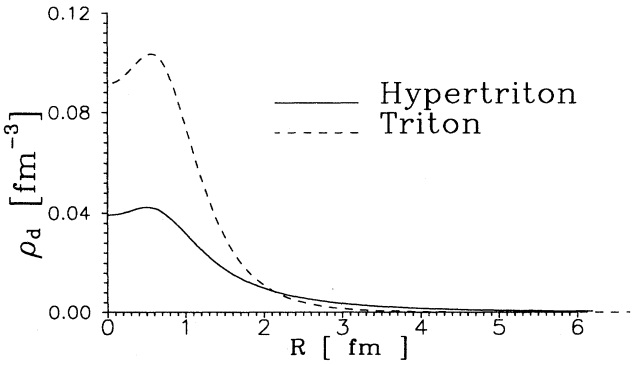

FIG. 11. Comparison of the deuteron overlap functions $\rho_d(r)$ for the triton and the hypertriton.

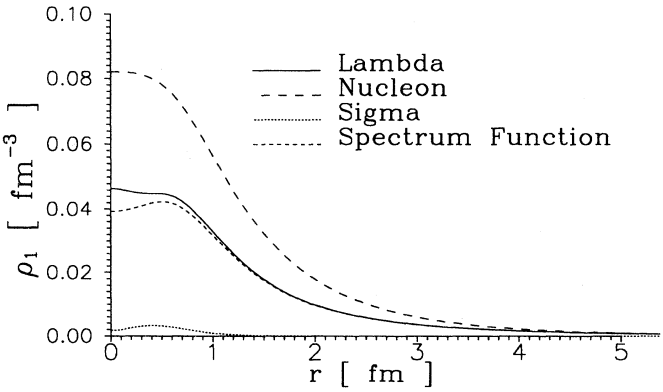

FIG. 12. The single-particle densities for the nucleon, the Λ, and the Σ in the hypertriton. The deuteron overlap function $\rho_d(r)$ of Fig. 11 is also shown.

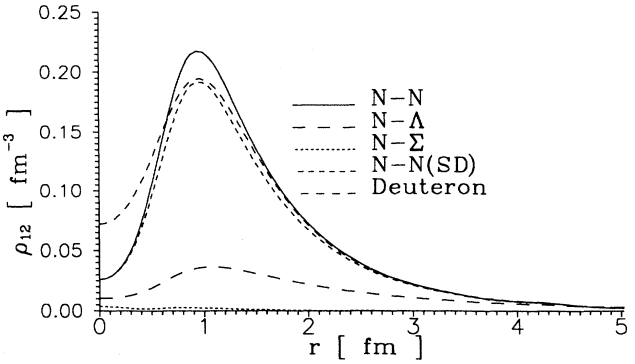

FIG. 13. The central correlation functions for the NN, ΛN, and ΣN pairs in the hypertriton, in comparison to the one in the deuteron. The NN correlation function in the hypertriton restricted to the $^3S_1$-$^3D_1$ state is also displayed.

potential. The two radial functions $\rho_d(r)$ are plotted in Fig. 11. While the one for the triton drops fast, the one for the hypertriton reaches out much further. Evaluating the normalizations

$$P_d \equiv \int_0^\infty dr r^2 \rho_d(r) \ , \tag{13}$$

we find $P_d = 0.448$ for the triton and $P_d = 0.987$ for the hypertriton, which substantiates the expectation mentioned above.

One step further we regard the single-particle density, i.e., the probability function to find a particle at a distance r from the center of mass. We display in Fig. 12 these quantities for the Λ and the nucleon. The Λ curve is of course very similar to the Λ curve in Fig. 11 (also shown) since the two nucleons have a high probability to be in the state of the deuteron inside the hypertriton. Finally, the Σ curve drops very quickly and is of course strongly suppressed.

Lastly, we show in Fig. 13 the two-body (central) correlation functions for an NN pair, a ΛN pair, and a ΣN pair. The NN correlation function is similar to the one for the deuteron (also shown), except that at very small distances the nucleons have smaller probabilities in the hypertriton than in the deuteron. The ΛN correlation function has of course a larger range and is flatter. At short distances ($r \leq 1$ fm) the NN correlation function is stronger suppressed in relation to its maximum than the one for the ΛN pair. That ratio for the deuteron is about in between. The ΣN correlation function does not show a suppression at short distances. Finally, the NN correlation function, when restricted to the $^3S_1$-$^3D_1$ state, is very similar to the one of the deuteron except at very short distances where it follows the full NN correlation function.

V. SUMMARY AND OUTLOOK

We solved the (matrix) Faddeev equations for the hypertriton using the Nijmegen hyperon-nucleon interac-

tion with full inclusion of the Λ-Σ conversion. The specific choice among the present day realistic *NN* forces is unimportant. We used the Nijmegen 93, Paris, and Bonn B interactions as examples. In all cases the hypertriton turned out to be bound at the experimental binding energy. We found that the Λ-Σ conversion is crucial for the binding of the hypertriton. This is obvious from Table II, where the total potential energy is broken apart into its various contributions. It is also of interest to note that the contribution of the $^1S_0$ and $^3S_1$-$^3D_1$ *YN* forces to the binding are not in the ratio 3:1 as often quoted, but are comparable.

The Jülich *YN* potential (the energy-independent $\tilde{A}$ version) does not lead to a bound hypertriton, as we showed in [1]. One reason might be the weaker attraction of the Jülich potential at very low energies of up to a few MeV, which corresponds to the typical kinetic energy of the Λ particle in the hypertriton. But also the Λ-Σ conversion potentials are very different in the Jülich case; see Table IV in comparison to Table II.

States of the Λ(Σ)*NN* system with quantum numbers (T, J) different from $(0, \frac{1}{2})$ are not bound.

Finally we visualized the hypertriton wave function in various manners including most probable spatial distributions of the three baryons, single baryon densities, and baryon-baryon correlation functions.

In the future it might be possible to measure nonmesonic and mesonic decays of the hypertriton or even hyperon-deuteron scattering. This will be a beautiful laboratory to (a) test weak processes in an interacting few-baryon system in a controlled manner, since not only the hypertriton but also the final three-nucleon continuum can be treated exactly, and (b) to study the energy dependence of the Λ-Σ conversion from the Λ*d* to the Σ*d* threshold and beyond. Theoretical studies in that direction are planned.

ACKNOWLEDGMENTS

This work has been supported by the Deutsche Forschungsgemeinschaft (H.K.) and the Australian Research Council (V.S.). The numerical calculations have been carried through on the CRAY Y-MP/832 of the Höchstleistungsrechenzentrum in Jülich. V.S. would like to thank Dr. Th.A. Rijken for helpful discussions on the momentum-space Nijmegen *YN* potential.

[1] K. Miyagawa and W. Glöckle, Phys. Rev. C **48**, 2576 (1993).
[2] A.G. Reuber, K. Holinde, and J. Speth, Czech. J. Phys. **42**, 1115 (1992).
[3] P.M.M. Maessen, Th.A. Rijken, and J.J. de Swart, Phys. Rev. C **40**, 2226 (1989).
[4] K. Ogawa, H. Narumi, and Y. Sunami, Prog. Theor. Phys. **63**, 533 (1980); J. Dabrowski and E. Fedorynska, Nucl. Phys. **A210**, 509 (1973); A.J. Toepfer and L.H. Schick, Phys. Rev. **175**, 1253 (1968).
[5] V.G.J. Stoks, R.A.M. Klomp, C.P.F. Terheggen, and J.J. de Swart, Phys. Rev. C **49**, 2950 (1994).
[6] Th.A. Rijken, R.A.M. Klomp, and J.J. de Swart, in *Essays in Celebration of the Life of Robert Eugene Marshak*, edited by E.C.G. Sudarshan (World Scientific, Singapore, 1995).
[7] R. Machleidt, Adv. Nucl. Phys. **19**, 189 (1989).
[8] M. Lacombe, B. Loiseau, J.M. Richard, R. Vinh Mau, J. Côté, P. Pirès, and R. de Tourreil, Phys. Rev. C **21**, 861 (1980).
[9] K. Miyagawa and W. Glöckle, to appear in Proceedings of the XIV International Few-Body Conference, Williamsburg, 1994.
[10] K. Miyagawa and W. Glöckle, to appear in Proceedings of the International Conference on Hypernuclear and Strange Particle Physics, Vancouver, 1994.
[11] The code we used was obtained from Dr. Y. Yamamoto and is a preliminary version of the Nijmegen soft-core *YN* potential. In this version some of the potential parameters are different from the values in the final version, as published in Phys. Rev. C **40**, 2226 (1989).
[12] G. Alexander, U. Karshon, A. Shapira, G. Yekutieli, R. Engelmann, H. Filthuth, and W. Lughofer, Phys. Rev. **173**, 1452 (1968).
[13] B. Sechi-Zorn, B. Kehoe, J. Twitty, and R.A. Burnstein, Phys. Rev. **175**, 1735 (1968).
[14] A. Stadler and B.F. Gibson, Phys. Rev. C **50**, 512 (1994).
[15] W. Glöckle, H. Witała, H. Kamada, D. Hüber, and J. Golak, to appear in Proceedings of the XIV International Few-Body Conference, Williamsburg, 1994 [9].